# High temperature solid oxide fuel cell integrated with novel allothermal biomass gasification: Part II: Exergy analysis

**Article** *in* Journal of Power Sources · September 2006

Impact Factor: 6.22 · DOI: 10.1016/j.jpowsour.2005.11.040



**5 authors**, including:

Kyriakos D Panopoulos
The Centre for Research and Technology, H...
**59** PUBLICATIONS **851** CITATIONS
SEE PROFILE

Lydia Fryda
Energy Research Centre of the Netherlands
**28** PUBLICATIONS **648** CITATIONS
SEE PROFILE

Available online at www.sciencedirect.com
ScienceDirect
Journal of Power Sources 159 (2006) 586–594
JOURNAL OF POWER SOURCES
www.elsevier.com/locate/jpowsour

# High temperature solid oxide fuel cell integrated with novel allothermal biomass gasification Part II: Exergy analysis

K.D. Panopoulos [a], L. Fryda [a], J. Karl [b], S. Poulou [c], E. Kakaras [a,*]

[a] *Laboratory of Steam Boilers and Thermal Plants, School of Mechanical Engineering, Thermal Engineering Section, National Technical University of Athens, 9 Heroon Polytechniou Ave. Zografou 15780, Greece*
[b] *Institute of Thermal Power Systems, Technical University of Munich, Boltzmannstrasse 15, 85747 Garching, Germany*
[c] *Hyperion Systems Engineering Ltd, Nicosia 1075, Cyprus*

Received 17 March 2005; received in revised form 8 November 2005; accepted 9 November 2005
Available online 27 December 2005

**Abstract**

Biomass gasification derived gas is a renewable fuel, which can be used for SOFC applications. This work investigates the integration of a near atmospheric solid oxide fuel cell (SOFC) with a novel allothermal biomass steam gasification process into a combined heat and power (CHP) system of less than $MW_e$ range. Heat for steam gasification is supplied from SOFC depleted fuel in a fluidised bed (FB) combustor via high temperature sodium heat pipes. In the first paper, the integrated system was modelled in Aspen Plus™ and critical aspects for its feasibility were identified.

The aim of this second part is the evaluation of the integrated system in exergy terms. Satisfying allothermal gasification heat demand is illustrated by examining each sub-process involved separately as well as combined. For a relatively low STBR = 0.6, the SOFC fuel utilisation for which the system operates under optimum conditions is $U_f = 0.7$. Above that value additional biomass has to be used in the FB combustor to provide gasification heat with considerable exergy losses. For SOFC operation at current density 2500 A $m^{-2}$, the system uses 90 kg $h^{-1}$ biomass, operates with electrical exergetic efficiency 32% producing 140 $kW_e$, while the combined electrical and thermal exergetic efficiency is 35%.


*Keywords:* Modelling; SOFC; Biomass; Gasification; Aspen Plus™; Exergy

## 1. Introduction

Available options for biomass CHP systems in the output range of 1 $MW_e$ include internal combustion engines, micro gas turbines and high temperature fuel cells (molten carbonate fuel cells, MCFCs or solid oxide fuel cells, SOFCs). The first commercial SOFC systems will be around 1 $MW_e$ nominal output, and their integration with biomass gasification in advanced small-scale configurations has gained attention recently [1,2].

When new power cycles are proposed, exergy analysis helps to identify the location, source, and magnitude of true losses in energy conversion operations, and finally, establish more effective systems. Prins and Ptasinski [3] compared the exergy losses of biomass gasification and combustion, and investigated the source of exergy losses in both processes. Bedringås et al. [4] analysed exergetically two methane fuelled SOFC systems, with limiting fuel utilisation factor of 0.75 due to pre-heating and methane reforming requirements. Monanteras and Frangopoulos [5] studied the performance of a SOFC system using the Pinch method with exergy analysis. Oostenkamp [6] performed a fuel cell system energy and exergy analysis using Aspen Plus™, and presented their results in Sankey and Grassmann diagrams. De Groot [7] presented in his thesis an exergy analysis of SOFC. Chan et al. [8] examined pressurised SOFC systems focusing on thermodynamic modelling and exergetic evaluation.

This Part II presents the exergetics of an advanced bioenergy SOFC–CHP system within 1 $MW_e$ range, using a novel allothermal steam gasification reactor called Biomass Heat Pipe Reformer (BioHPR) [9]. The energy and exergy evaluation is based on Part I's steady state model built in Aspen Plus™

* Corresponding author. Tel.: +30 210 7723662; fax: +30 210 7723663.
*E-mail address:* ekak@central.ntua.gr (E. Kakaras).

0378-7753/$ – see front matter © 2005 Elsevier B.V. All rights reserved.
doi:10.1016/j.jpowsour.2005.11.040

**Nomenclature**

| | |
|---|---|
| $E$ | total exergy of a material stream (product gas, char, biomass, additional biomass, air, steam) (W) |
| $E_T^Q$ | thermal exergy of a heat steam available at temperature $T$ (W) |
| $E^W$ | work or power output (W) |
| FB | fluidised bed |
| $h$ | enthalpy of a stream (J mol$^{-1}$) |
| $h_{fg}$ | = 2442 kJ kg$^{-1}$; latent heat of water vaporisation |
| $h_0$ | standard enthalpy at environmental conditions ($T_0$, $p_0$) (J mol$^{-1}$) |
| $I$ | irreversibility (W) |
| LHV | low heating value (kJ kg$^{-1}$ for solids/MJ $m_n^{-1}$ for gases) |
| $LHV_{fuel,dry}$ | = 17,567 kJ kg$^{-1}$; low heating value of dry fuel |
| $N$ | mole flow rate (mole s$^{-1}$) |
| $p$ | pressure (bar) |
| $P_{SOFC}$ | direct current electric power produced from the SOFC (W) |
| $Q$ | heat stream (W) |
| $Q_{req}$ | required heat for allothermal gasification (W) |
| $R$ | = 8314 J mol$^{-1}$ K; ideal gas constant |
| $s$ | entropy of a stream (J mole$^{-1}$ K) |
| $s_0$ | standard entropy at environmental conditions ($T_0$, $p_0$) (J mol$^{-1}$) |
| STBR | steam to biomass ratio (refers to gasification) |
| STCR | steam to carbon ratio (refers to SOFC operation) |
| $T$ | temperature (K) |
| $U_f$ | SOFC fuel utilisation factor |
| $w$ | moisture mass fraction in fuel (w/w) |
| $x_i$ | mole fraction of component $i$ |
| $z_C$, $z_{H_2}$, $z_{O_2}$, $z_{N_2}$ | mass fraction of carbon, hydrogen, oxygen and nitrogen in dry fuel |

*Greek symbols*

| | |
|---|---|
| $\eta$ | efficiency |
| $\eta_c$ | Carnot efficiency |
| $\eta_{ex,gas}$ | exergetic efficiency of gasification |
| $\eta_{ex,HP}$ | exergetic efficiency of heat pipe operation |
| $\varepsilon_{ch}$ | specific (molar) chemical exergy of a material stream (J mole$^{-1}$) |
| $\varepsilon_{ch,fuel}$ | fuel chemical exergy (kJ kg$^{-1}$) Eq. (4) |
| $\varepsilon_{0,i}$ | standard chemical exergy of a component $i$ in a mixture |
| $\varepsilon_{ph}$ | specific (molar) physical exergy of a material stream (J mole$^{-1}$) |

*Subscripts*

| | |
|---|---|
| biomass, add. biomass | additional biomass in the FB combustor |
| cg | cold gas |
| char | char produced during gasification, modelled as graphite $C_{(s)}$ |
| CHP | combined heat and power overall system |
| comb | combustion |
| depleted gas/air | not spent product gas/air in the SOFC stack, output material stream from the SOFC stack |
| el | electrical |
| ex | exergetic |
| gas | gasification |
| HP | heat pipes |
| heat | used in Eq. (15) to denote combustion efficiency for available thermal exergy towards gasification |
| $j$, $k$ | subscripts denoting ingoing and outgoing material stream components respectively in a control volume |
| SOFC | solid oxide fuel cell stack |

process simulation software in which four major subsections are incorporated: gasification, heat pipes, SOFC, and gas cleaning. The first three together with recuperative heat exchangers are parts of the overall thermal integration attempted. Second law efficiencies are defined for the major process steps and presented parametrically while the overall CHP exergy efficiency is analysed and a base case is presented in a Grassmann diagram.

## 2. System configuration

The proposed CHP system flowchart, also described in Part I, consists of two fluidised bed reactors thermally coupled by means of heat pipes, a product gas cleaning train, a SOFC stack and its power conditioning, an air blower compressor, two gas-to-gas heat exchangers (HX1 and 2), a heat recovery steam generator (HX3), and (HX4) producing hot water (Fig. 1). The gasifier and combustion FBs operate at 1073 K, ∼1.5 bar and 1173 K, ∼1.1 bar respectively. This allows a temperature difference of 100 K for heat transfer with the integrated sodium heat pipes to provide thermal energy requirements for the allothermal gasification. The hot product gas stream enters a gas-to-gas heat exchanger (HX1) where it cools down to 670 K by preheating the clean product gas, while further spontaneous heat dissipation to the environment drops product gas temperature further. Pressure drops and thermal losses for each unit operation were assumed 2%. Particulates are removed by a barrier-type filter and halogen and sulphide removal is accomplished in high temperature sorbent trap beds. The gas cleaning takes place at temperatures above tar dew point. The desired gas temperature is achieved by proper piping insulation and temperature control. The cleaned gas is reheated in HX1 and then into a compact tar-cracking reactor placed inside the combustion FB, where product gas temperature rises to 1123 K. Additional steam is then added, increasing the gaseous fuel water content to avoid carbon deposition on the SOFC anode. Air is blown to the near atmospheric SOFC operating pressure and heated up to 900 K in HX2 before entering the stack. Depleted fuel and air from the SOFC are combusted in the secondary FB together with gasification by-product char. Additional biomass can be combusted if the above

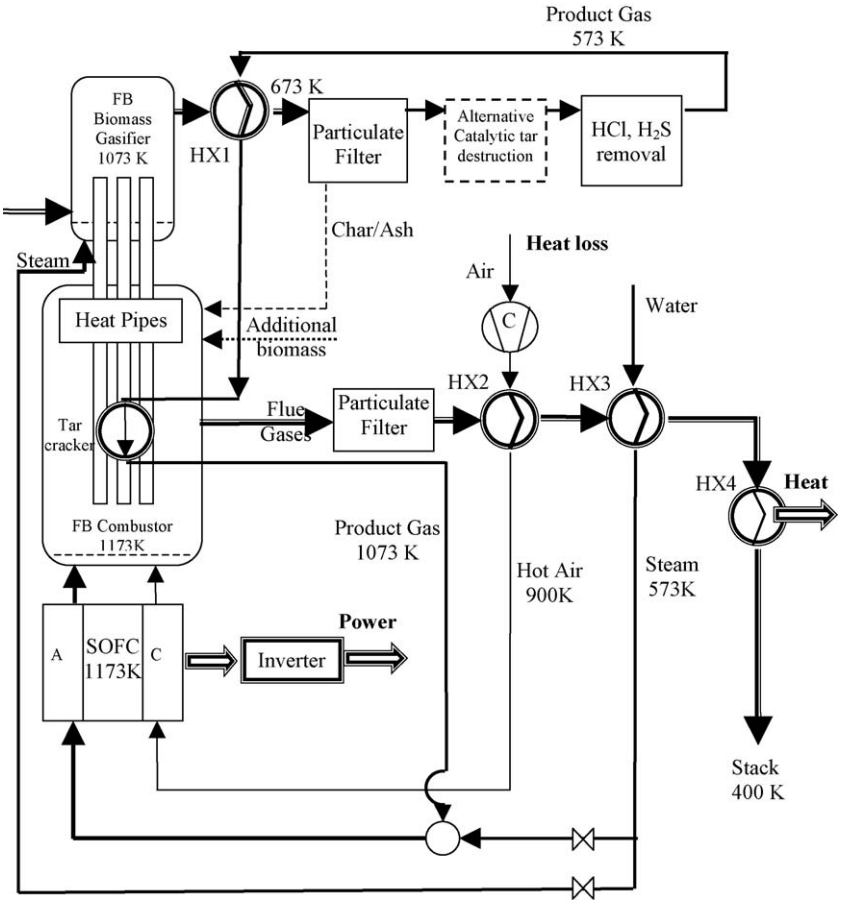


Fig. 1. Flowchart of the combined SOFC/allothermal biomass gasification CHP.

are not enough to sustain gasification. The flue gas thermal content is recuperated in HX2, followed by a heat recovery steam generator (HRSG) HX3, providing steam for the gasification and product gas moistening. Finally, HX4 offers useful heat in the form of hot water around 360 K. An inverter provides alternating current electrical power. The capacity of the system studied is based on a SOFC with 100 $m^2$ active surface resulting in electrical outputs range of 100–200 $kW_e$. Nevertheless, the presented system is envisaged for up to 1 $MW_e$ size and an attempt to present size independent data has been made. Details relative to the assumptions for the modelling can be found in Part I of this work.

## 3. Exergy analysis

### 3.1. Methodology

Exergy is the maximum work that can be produced when a heat or material stream is brought to equilibrium relatively to a reference environment, which consists of reference components and is characterised by absence of pressure and temperature gradients. Exergy analysis of a process is a supplement to energy analysis, used to assess work potentials of input and output material and heat streams, and pinpoint irreversibility losses.

Exergy associated with a material stream is expressed as the sum of its physical and chemical exergy, corrected in case of deviation between actual environmental and reference conditions. In this study, no deviation was considered. Potential, kinetic and other types of exergy are neglected. The total exergy of a material stream is given by equation:

$$E = N(\varepsilon_{ph} + \varepsilon_{ch}) \quad (W) \tag{1}$$

where $N$ is the flow rate in mol $s^{-1}$. The molar physical exergy of a material stream is expressed in relation to the reference environmental conditions as:

$$\varepsilon_{ph} = (h - h_0) - T_0(s - s_0) \quad (J\ mol^{-1}) \tag{2}$$

Mole flows, mole fractions, enthalpy and entropy of each material stream were taken from the Aspen Plus™ flow sheet results. For every material stream, duplication was created and brought to standard environmental conditions for the evaluation of its molar reference enthalpy and entropy ($h_0$, $s_0$). The standard environmental conditions of Aspen Plus™ ($T_0 = 298.15$ K, $p_0 = 1.013$ bar) were adopted as reference conditions in the study.

The molar chemical exergy of a gaseous material mixture is given by:

$$\varepsilon_{ch,gas} = \sum_i x_i \varepsilon_{0,i} + RT_0 \sum_i x_i \ln x_i \quad (J\,mol^{-1}) \tag{3}$$

where $x_i$ is the mole fraction and $\varepsilon_{0,i}$ is the standard molar chemical exergy of each component $i$, in J $mol^{-1}$. The latter are given

in tables [10,11] based on slightly different assumptions for the reference atmospheric composition. In the present study, values given by Kotas [10] were used. The chemical exergy of solid fuel was calculated with the help of the statistical correlation $\beta$, proposed by Szargut et al. [11]:

$$\varepsilon_{\text{ch, solid}} = (\text{LHV}_{\text{fuel, dry}} + wh_{\text{fg}})\beta \quad (\text{kJ kg}^{-1}) \tag{4}$$

The biomass fuel considered was olive kernel residues, the proximate and ultimate analysis of which was presented in Part I. The fuel oxide to carbon mass fraction falls within $0.667 \leq (z_{O_2}/z_C) \leq 2.67$, and the formula of $\beta$ for wood is applied [11]:

$$\beta = \frac{1.0412 + 0.216(z_{H_2}/z_C) - 0.2499(z_{O_2}/z_C)[1 + 0.7884(z_{H_2}/z_C)] + 0.045(z_{N_2}/z_C)}{1 - 0.3035(z_{O_2}/z_C)} \tag{5}$$

where $z_i$ are the mass fraction ratios of elemental fuel components.

Using Eqs. (1)–(5), exergy is calculated for all material streams in the flow sheet. The exergy of a heat stream $Q$ is given with the help of the Carnot factor: $E_T^Q = Q(1 - T_0/T)$, where $T$ is the temperature at which $Q$ is available. Exergy of power output equals power itself. The exergy balance of a steady state process takes the following form:

$$\sum_{\text{IN}} E_j + \sum_{\text{IN}} E^Q_{T_{\text{IN}}} = \sum_{\text{OUT}} E_k + \sum_{\text{OUT}} E^Q_{T_{\text{OUT}}} + \sum_{\text{OUT}} E^W + I \tag{6}$$

where $\sum_{\text{IN}} E_j$ and $\sum_{\text{OUT}} E_k$ are the exergy flows of the in and out going material streams, $\sum_{\text{IN}} E^Q_{T_{\text{IN}}}$, $\sum_{\text{OUT}} E^Q_{T_{\text{OUT}}}$ the exergy flows of the in and useful out going heat streams at $T_{\text{IN}}$ and $T_{\text{OUT}}$, respectively, $\sum_{\text{OUT}} E^W$ the power produced in the process and $I$ the irreversibility that represents the loss of quality of materials and energy due to dissipation.

The main issue of the exergetic analysis is to investigate how efficient is the exergy transfer from the SOFC off gases and char combustion via heat pipes to allothermal gasification. The critical processes for this are: the gasification, heat transfer through heat pipes, SOFC operation and combustion, for which exergetic efficiencies are defined and examined parametrically in Sections 3.2–3.5, respectively.

### 3.2. Allothermal gasification exergy analysis

Allothermal biomass gasification transforms the solid primary fuel into a gaseous fuel with the addition of externally provided heat. Gasification temperatures range between 973 and 1173 K, which means that the heat source must be kept at a higher temperature so as to maintain the necessary heat transfer rate. For this purpose, in practice allothermal gasification is performed in double gasification/combustion FBs taking advantage of their increased heat transfer capabilities. In the present work, this is accomplished by means of high temperature heat pipes. The control volume for the isolated gasification process analysis is presented in Fig. 2. In order to estimate the outlet composition and thermal requirements of the process, a simple gasification model was built based on the following assumptions:

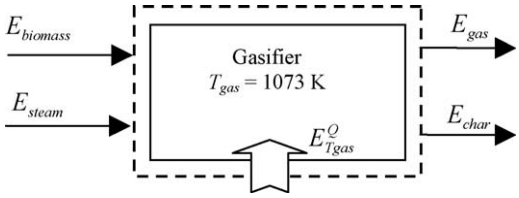


Fig. 2. Gasification control volume.

- Char and hydrocarbons are not predicted thermodynamically.
- Product char was modelled as graphite $C_{(s)}$ and was assumed 10% of the biomass carbon input.
- Methane in the product gas outlet was allowed to range from 5 to 10% deriving from 10% of the initial carbon input.
- Tar was included to up 5 g $m_n^{-3}$ in dry basis product gas.
- The remaining elemental composition of biomass and steam were assumed at thermodynamic equilibrium of $C_{(s)}$, $H_2$, CO, $CO_2$, $CH_4$ and $H_2O$.

Apart from biomass analyses, parameters affecting the product gas composition are temperature, pressure and steam to biomass ratio (STBR):

$$\text{STBR} = \frac{\text{Steam + fuel moisture } (\text{kg s}^{-1})}{\text{Dry biomass } (\text{kg s}^{-1})} \tag{7}$$

Gasification temperature and pressure were decided $T_{\text{gas}} = 1073$ K, and $p_{\text{gas}} = 1.5$ bar and were not used as parameters. Slightly altered temperatures have little influence on the product gas composition. Significant gasification temperature increase would inhibit effective heat transfer from an external source. Without any additional compressing, the pressure level was chosen so as to overcome subsequent pressure drops during gas cleaning, SOFC, secondary FB combustor and heat recovery exchangers, up to flue gas disposal. The main parameter investigated for its influence on the gasification effectiveness was the STBR.

Amongst several useful output-to-input ratios that can be defined for the expression of solid fuel gasification process efficiency, the most common is the cold gas efficiency, $\eta_{\text{cg}}$, neglecting the sensible heat of the produced gas [12]:

$$\eta_{\text{cg}} = \frac{\text{LHV in product gas}}{\text{LHV in feedstock}} \tag{8}$$

The term "LHV in product gas", does not include char (modelled as graphite, $C_{(s)}$), which is a by-product not directly useful for subsequent power production. Based on this definition, allothermal gasification cold gas efficiency could reach values beyond unity because externally supplied thermal energy is not taken into account. Alternatively, allothermal gasification efficiency can take into account the required heat for the endothermic gasification process $Q_{\text{req}}$:

$$\eta'_{\text{cg}} = \frac{\text{LHV in product gas}}{\text{LHV in feedstock} + Q_{\text{req}}} \tag{9}$$

Usually $Q_{req}$ is delivered by combusting a secondary fuel and it is commonly replaced in Eq. (9) by the corresponding LHV input. In the present study, symbol $Q_{req}$ was kept for consistency with the gasification control volume of Fig. 2.

In Eqs. (8) and (9), the product gas sensible heat was not considered. Most important drawback in these two definitions is that the entropy increase due to conversion of a solid fuel to a gaseous one is not considered [13]. Exergetic efficiency avoids these drawbacks. Based on the general definition of the degree of perfection for a process by Szargut et al. [11], the exergetic efficiency of allothermal gasification is:

$$\eta_{ex,gas} = \frac{E_{gas} + E_{char}}{E_{biomas} + E^{Q}_{T_{gas}} + E_{steam}} \quad (10)$$

where $E_{gas} + E_{char}$ the outgoing (product) exergy streams, $E_{biomass}$ and $E_{steam}$ the incoming fuel and steam exergies, and $E^{Q}_{T_{gas}}$ is the exergy of the heat input available at $T_{gas}$. $E^{Q}_{T_{gas}}$ is the product of $Q_{req}$ multiplied with the Carnot efficiency at $T_{gas}$, $\eta_c = 1 - T_0/T_{gas}$. Steam is introduced to the gasification process at 573 K and 2 bar. Only the chemical exergy of solid char is included in $E_{char}$ because its physical exergy is minor in comparison.

With increasing STBR, the cold gas efficiency (using Eq. (9)) is maximised when carbon conversion is maximised up to the point where the gasification model allows and decreases slowly thereafter (Fig. 3). From that point onward, additional $Q_{req}$ is mostly consumed to bring larger steam flows at the gasification temperature rather than enhance fuel species production. The exergetic efficiency decrease is continuous with STBR and steeper due to the combination of: (a) product gas exergy decrease caused by water vapour dilution and (b) larger thermal exergy requirements. Therefore, from a thermodynamic point of view, biomass allothermal gasification processes should be realised with the minimum steam necessary for maximising carbon conversion. Similar conclusions are found in literature based on experiments [14].

Nevertheless, kinetic reasons such as pushing towards completion of tar reforming reactions, or fluidisation limitations might pose higher STBR in practice. On the other hand, as it was shown in Part I of the work, gas cleaning of $H_2S$ at high temperatures is inhibited by high water vapour concentrations. STBR = 0.6 was adopted in the overall system study. Additional steam must, therefore, be supplied to the product gas after gas cleaning, to achieve a carbon deposition free SOFC operation assumed at steam to carbon ratio STCR = 2.

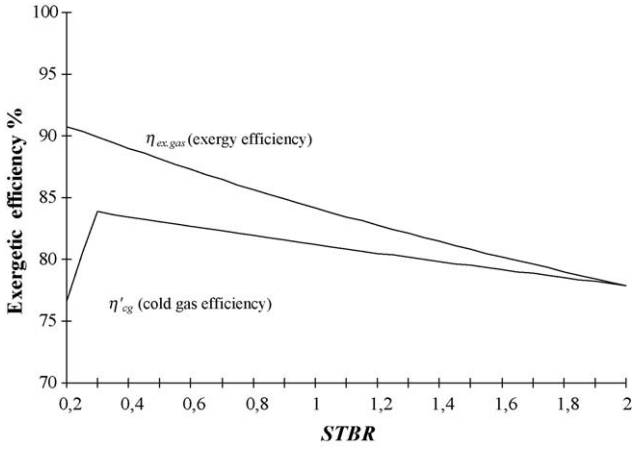


Fig. 3. Cold gas efficiency and exergetic efficiency of allothermal gasification vs. STBR at $T_{gas}$ = 1073 K, and $p_{gas}$ = 1.5 bar.

### 3.3. Heat transfer through heat pipes exergy analysis

The heat transfer across heat pipes is examined versus the control volume defined in Fig. 4. Heat pipes receive heat at $T_{comb}$ = 1173 K combustor temperature and deliver it at $T_{gas}$ = 1073 K gasification temperature. The heat transfer exergetic efficiency for the heat pipes is evaluated as:

$$\eta_{ex,HP} = \frac{E^{Q}_{T_{gas}}}{E^{Q}_{T_{comb}}} \quad (11)$$

which results in:

$$\eta_{ex,HP} = \frac{(T_{gas} - T_0)T_{comb}}{(T_{comb} - T_0)T_{gas}} \quad (12)$$

with $E^{Q}_{T_{gas}} = Q_{req}(1 - T_0/T_{gas})$ and $E^{Q}_{T_{comb}} = Q_{req}(1 - T_0/T_{comb})$, the exergy of the heat streams at gasification and combustion temperatures respectively and $T_0$ the reference environmental temperature set at 298.15 K. For the defined operating temperatures, $\eta_{ex,HP}$ = 96.8%. Larger number of heat pipes, i.e. larger heat transfer area, and thus, reduced required $T_{comb}$ would result in higher exergetic efficiencies at the expense of additional costs for heat pipes purchase. It is noted that in energetic terms, the efficiency of heat transferred is 100%.

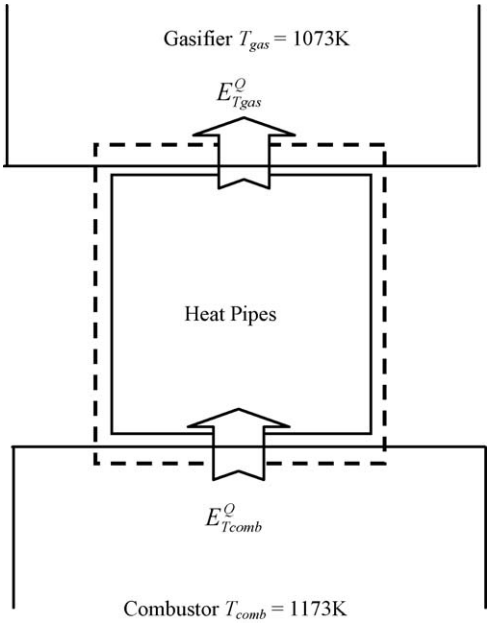


Fig. 4. Heat pipe control volume.

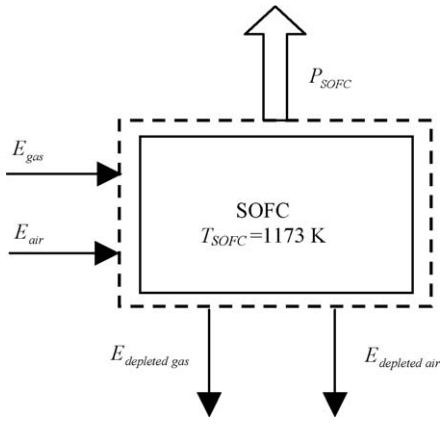


Fig. 5. SOFC control volume.

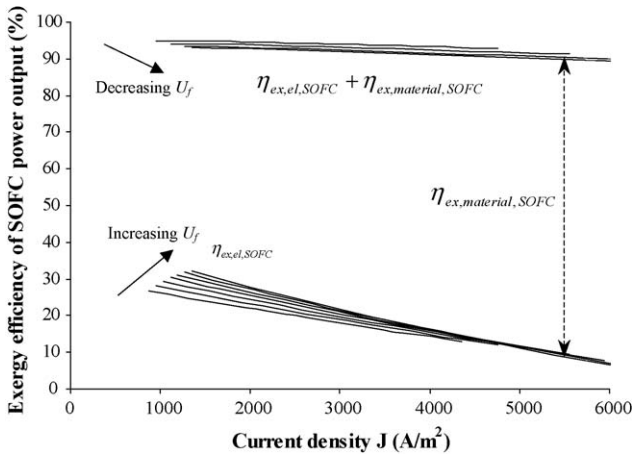


Fig. 6. SOFC electrical, material and overall exergetic efficiency vs. fuel utilisation for various primary biomass inputs.

### 3.4. SOFC exergy analysis

Fuel cells convert fuel chemical energy to power more efficiently than heat engines. The electron movement in fuel cell chemical reactions is more controlled and part of electron bonding energy is extracted electrically, whereas in combustion the energy released is totally converted towards thermal energy [15,16].

The control volume for the exergetic analysis of the SOFC is shown in Fig. 5. The operating SOFC temperature is set at $T_{SOFC} = 1173$ K, moistened product gas enters at approximately 1073 K and air at 900 K. Both anode and cathode outgoing streams are introduced directly to the secondary FB combustor. The main feature of this SOFC operation is the absence of an integrated post combustor chamber that usually transfers heat to incoming air. The present configuration results to slightly reduced airflows and incoming air has to be internally heated up closer to cathode temperature by available dissipated SOFC heat. The SOFC model, described in Part I of this work, was built in Aspen Plus$^{TM}$ using available unit operation blocks and FORTRAN calculators to estimate its electrochemical parameters.

The exergetic electrical efficiency of the SOFC is defined as the ratio of net electric power output of the SOFC, to input material streams exergy:

$$\eta_{ex,\,el,\,SOFC} = \frac{P_{SOFC}}{E_{gas} + E_{air}} \tag{13}$$

One more ratio is defined, expressing the total output material stream exergy to input material streams exergy:

$$\eta_{ex,\,material,\,SOFC} = \frac{E_{depleted\,gas} + E_{depleted\,air}}{E_{gas} + E_{air}} \tag{14}$$

The total SOFC exergetic efficiency is the sum of Eqs. (13) and (14). Eq. (13) illustrates the efficiency of the SOFC for its primary purpose to deliver power. Eq. (14) shows the effectiveness of the SOFC in delivering exergy to be used for covering gasification thermal requirements. Fig. 6 shows these efficiencies against current density for several fuel utilisation values. Increasing primary biomass feed rate increases fuel gas flow rate and consequently, SOFC current densities, voltage drops, and thus electrical exergetic efficiency decreases. Electrical exergy efficiencies reach an optimum and then decrease with fuel utilisation. The optimum point is shifted towards larger $U_f$ values, as the SOFC gas fuel input decreases. For small fuel gas inputs, electrical exergetic efficiencies do not drop practically at all within the specified range of fuel utilisation. This tendency is expected because overpotentials remain low for small $U_f$ and fuel gas inputs. The total SOFC exergetic efficiency decreases with fuel utilisation factor because of the increased conversion of input fuel chemical exergy towards other forms.

### 3.5. Fluidised bed combustor exergy analysis

The control volume for the combustion of SOFC off gases and char is shown in Fig. 7. The combustion temperature is set at $T_{comb} = 1173$ K and heat is transferred to the gasifier via sodium heat pipes. This heat stream is the useful outcome of the combustor for covering gasification heat demand, so the efficiency is defined as:

$$\eta_{ex,\,heat,\,comb} = \frac{E^{Q}_{T_{comb}}}{E_{char} + E_{depleted\,air} + E_{depleted\,gas} + E_{add.biomass}} \tag{15}$$

The combustion efficiency largely depends on the depleted fuel gas. When $U_f$ is small, combustor available heat at 1173 K is large and $\eta_{ex,heat,comb}$ is high (Fig. 8). The SOFC operates with higher air throughput when larger amounts of fuel gas are used.

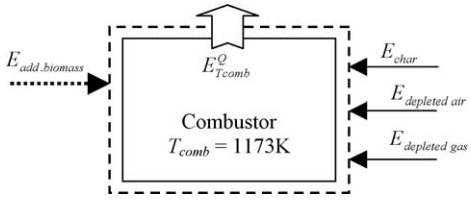


Fig. 7. Combustion control volume.

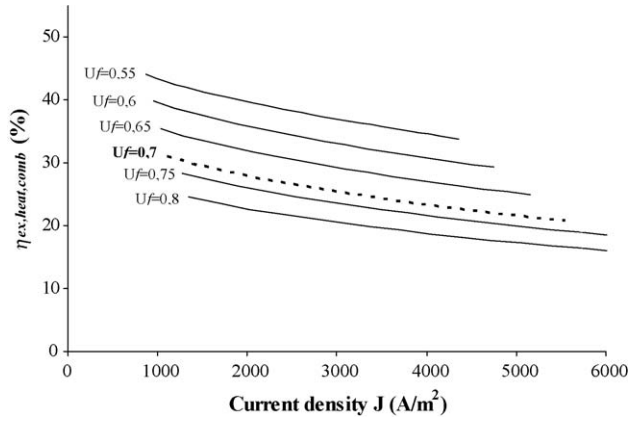


Fig. 8. Combustion exergetic efficiency for heat production at $T_{comb} = 1173$ K.

Large amounts of depleted air deteriorate the efficiency of the combustor.

## 4. Exergetic evaluation of the integrated gasification SOFC system

### 4.1. Providing allothermal gasification thermal exergy requirement

Exergetic results for individual processes described in Sections 3.2–3.5 can be combined into Fig. 9 illustrating how allothermal gasification heat exergy demand is satisfied by transferring exergy from SOFC off gases and char combustion via heat pipes. Up to fuel utilisation ~0.7 the outlet anode streams (depleted fuel and air) and char separated from the product gas, are sufficient to provide the requirements of gasification. Therefore, no additional biomass feeding to the combustor is necessary. Beyond $U_f > 0.7$, additional biomass fuel has to be supplied but its exergetic efficiency is restricted by large irreversibility.

If flue gas exergy is enough to sustain gasification, then the combustor FB could operate with an ash free fuel and subsequent gas cleaning and fouling of heat exchangers would be minimised. Char and ash could then be alternatively recirculated to the gasifier with a slip stream rejecting mostly ash.

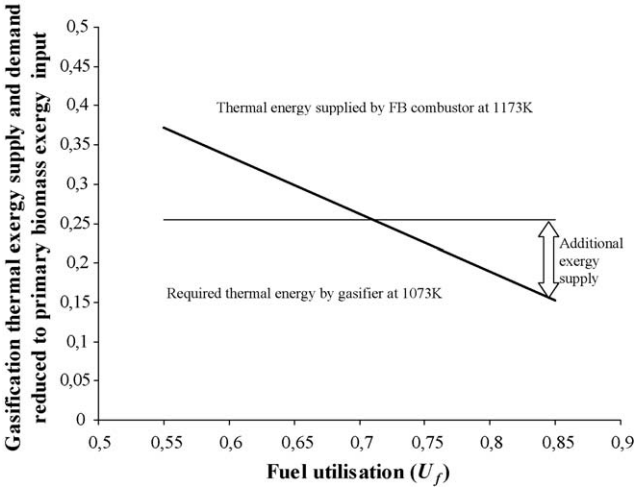


Fig. 9. Gasification thermal exergy supply and demand reduced to primary exergy input.

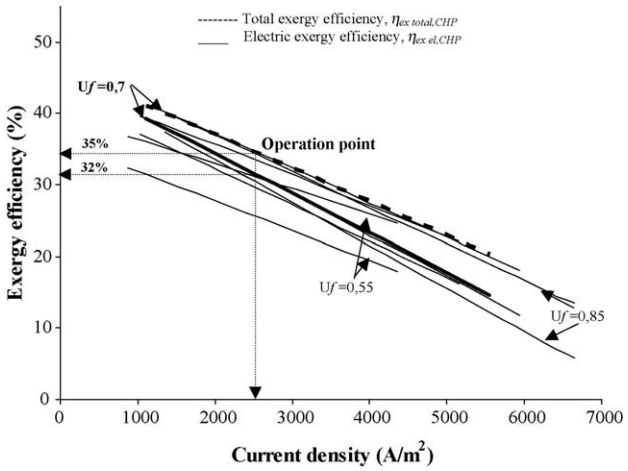


Fig. 10. CHP electrical and total exergetic efficiencies vs. current density for various primary biomass inputs.

### 4.2. Exergy analysis of the integrated system

The exergetic efficiency of the overall proposed CHP system for electricity production is:

$$\eta_{ex,el,CHP} = \frac{P_{SOFC}}{E_{biomass} + E_{add.\,biomass}} \quad (16)$$

The combined electrical and thermal exergetic efficiency of the proposed system is:

$$\eta_{ex,total,CHP} = \frac{P_{SOFC} + E^{Q}_{T_{STACK}}}{E_{biomass} + E_{add.\,biomass}} \quad (17)$$

where $E^{Q}_{T_{STACK}}$ the exergy of the heat produced in HX4 (Fig. 1) by the combustor flue gas stream prior to stack outlet. Fig. 10 shows total and electric exergy efficiencies against current densities. The efficiencies are maximum for $U_f = 0.7$, as beyond this

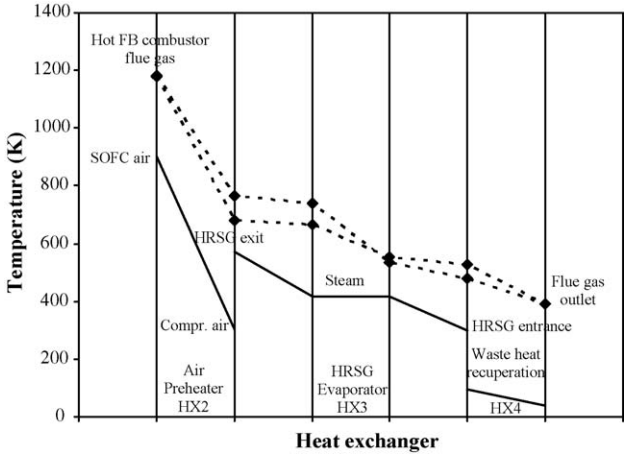


Fig. 11. Heat exchanger cold and hot side temperature differences.

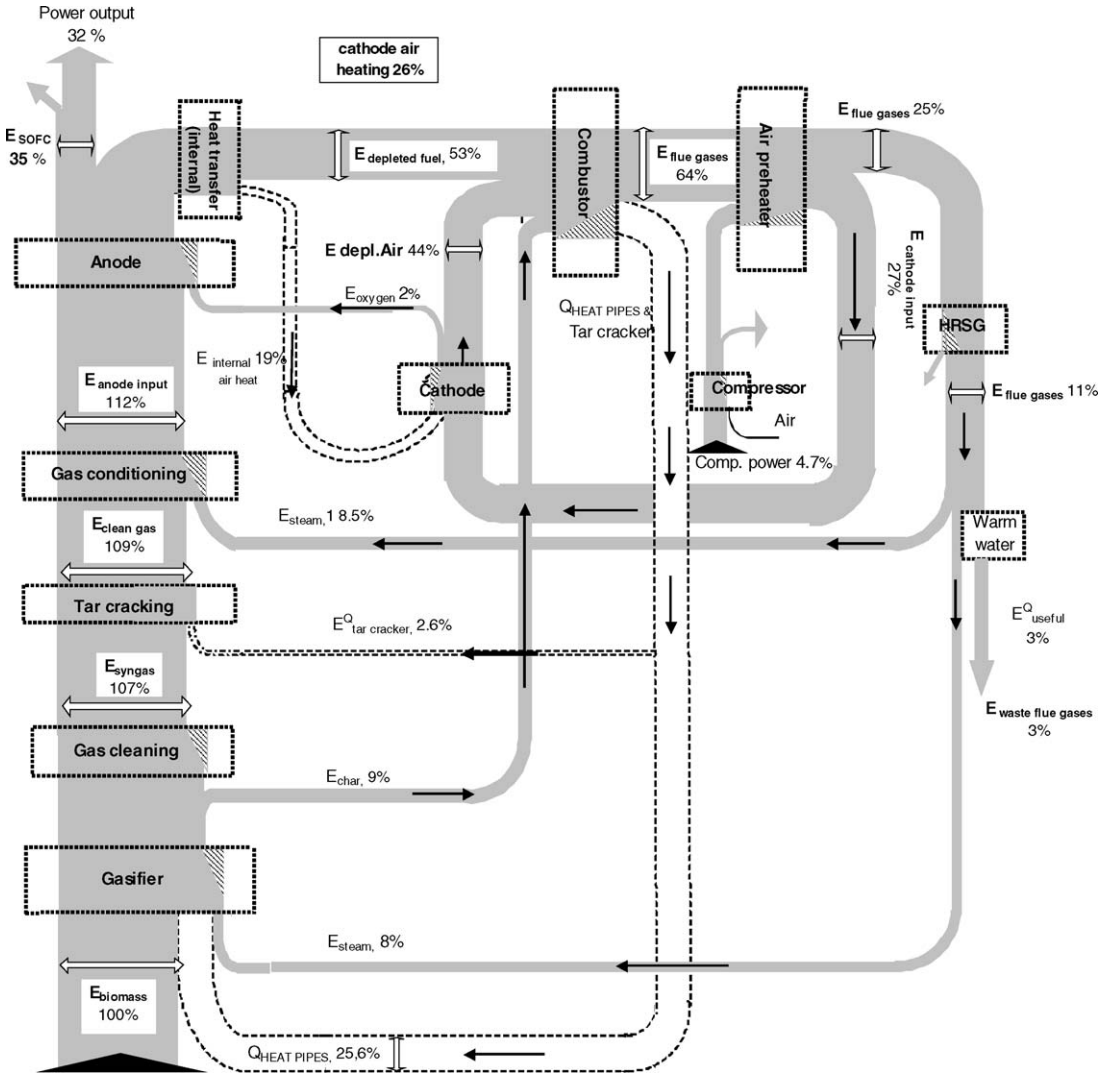


Fig. 12. Grassman diagram of the CHP–SOFC biomass gasification integrated system.

operation point additional biomass input into the combustor is necessary, which lowers efficiency.

For a large range of feeding rates and power outputs the system's efficiency is optimised for $U_f = 0.7$, which can be selected irrespectively of the design point nominal power output of the system, when this is optimised according to relative electricity and thermal conversion in respect with capital costs of equipment.

As far as recuperative heat exchangers are concerned, an attempt was made to present the analysis using relaxed $\Delta T_{min}$. For $U_f = 0.7$ and for the minimum and maximum primary biomass feed rates used the $\Delta T$s for HX2–HX4 are illustrated in Fig. 11 and are never less than 150 K. The CHP thermal output could be increased if smaller $\Delta T$s were adopted with higher exchanger surfaces and, therefore, capital costs.

For an average current density $J = 2500\ A\ m^{-2}$, at $U_f = 0.7$, the gasifier consumes $90\ kg\ h^{-1}$ biomass, the electrical exergetic efficiency is $\eta_{ex,el,CHP} = 32\%$ producing $P_{SOFC} = 140\ kW_e$, while the combined electrical and thermal exergetic efficiency is $\eta_{ex,total,CHP} = 35\%$. The complete analysis results are shown for this case in a Grassman diagram in Fig. 12.

## 5. Conclusions

The combination of allothermal biomass gasification and SOFC for small scale CHP was analysed exergetically using results from Part I of this work. The system operates near atmospheric pressure and is based on the novel BioHPR reactor, already proven for its capability to transfer required gasification heat between combustion and gasification fluidised beds by using high temperature heat pipes [9].

The effectiveness of providing allothermal gasification heat demand by transferring heat from SOFC off gases and char combustion via sodium heat pipes was illustrated by examining each sub-process separately as well as combined. For a relatively low STBR = 0.6, fuel utilisation $U_f$ for which the system operates under optimum conditions is 0.7. Above that value additional biomass has to be used in the combustion FB to provide gasification heat with great exergy losses.

For SOFC current density 2500 A $m^{-2}$, at $U_f = 0.7$, the system uses 90 kg $h^{-1}$ biomass, operates with electrical exergetic efficiency $\eta_{ex,el,CHP} = 32\%$ producing $P_{SOFC} = 140\,kW_e$, while the combined electrical and thermal exergetic efficiency is $\eta_{ex,total,CHP} = 35\%$.

## References


[1] S. Baron, N. Brandon, A. Atkinson, B. Steele, R. Rudkin, The impact of wood-derived gasification gases on Ni-CGO anodes in intermediate temperature solid oxide fuel cells, J. Power Sources 126 (2004) 58–66.

[2] O. Omosun, A. Bauen, N.P. Brandon, C.S. Adjiman, D. Hart, Modelling system efficiencies and costs of two biomass-fuelled SOFC systems, J. Power Sources 131 (2004) 96–106.

[3] M.J. Prins, K.J. Ptasinski, Energy and exergy analyses of the oxidation and gasification of carbon, Energy 30 (2005) 982–1002.

[4] K.W. Bedringås, I.S. Ertesvåg, S. Byggstøyl, B.F. Magnussen, Exergy analysis of solid-oxide fuel-cell (SOFC) systems, Energy 22 (1997) 403–412.

[5] N.C. Monanteras, C.A. Frangopoulos, Towards synthesis optimization of a fuel-cell based plant, Energy Convers. Manage. 40 (1999) 1733–1742.

[6] P.F. van den Oosterkamp, Review of an energy and exergy analysis of a fuel cell system, J. Power Sources 41 (1993) 239–252.

[7] A. de Groot, Advanced exergy analysis of high temperature fuel cell systems, PhD Thesis, Energy Research Centre of the Netherlands, Petten, 2004.

[8] S.H. Chan, C.F. Low, O.L. Ding, Energy and exergy analysis of simple solid-oxide fuel-cell power systems, J. Power Sources 103 (2002) 188–200.

[9] EU funded Project Biomass Heatpipe Reformer-Project, Acronym: BioHPR, Contract no. ENK5-CT-2000-0311, 2001–2004, available at: www.biohpr.de, Stand: 08, August 2005.

[10] T.J. Kotas, The Exergy Method of Thermal Plant Analysis, Krieger Publishing Company, Malabar, Florida, 1995.

[11] J. Szargut, D.R. Morris, F.R. Steward, Exergy Analysis of Thermal Chemical, and Metallurgical Processes, Taylor & Francis Inc., 1988.

[12] C. Higman, M. van der Burgt, Gasification, Gulf Publishing, 2003.

[13] M.J. Prins, K.J. Ptasinski, F.J.J.G. Janssen, Thermodynamics of gas–char reactions: first and second law analysis, Chem. Eng. Sci. 58 (2003) 1003–1011.

[14] H. Hofbauer, R. Rauch, Stoichiometric ater consumption of steam gasification by the FICFB-gasification process, in: A.V. Bridgwater (Ed.), Progress in Thermochemical Biomass Conversion, Vol. 1, Blackwell Science, Oxford, 2001, pp. 199–208.

[15] A.E. Lutz, R.S. Larson, J.O. Keller, Thermodynamic comparison of fuel cells to the Carnot cycle, Int. J. Hydr. Energ. 27 (2002) 103–111.

[16] S.E. Wright, Comparison of the theoretical performance potential of fuel cells and heat engines, Renew. Energ. 29 (2004) 179–195.